Cancer Nanotechnology

RESEARCH Open Access

Investigation of hollow mesoporous $NiFe_2O_4$ nanospheres fabricated via a template-free solvothermal route as pH-responsive drug delivery system for potential anticancer application

Qing Qi[1], Hui Zhang[1], Mengru Liu[1], Shujing Qi[1*], Zhongchao Huo[1], Yingying Ma[2], Zhongqiang Zhang[3], Yongchang Lu[3*], Xiongwei Qi[2], Shuai Han[2] and Guangshuo Wang[2*]

*Correspondence:
365243811@qq.com;
lych1023@163.com;
wgs8136@163.com

[1] Cancer Center, Affiliated Hospital, Hebei University of Engineering, Handan 056002, Hebei, China
[2] Key Laboratory of New Inorganic Nonmetallic Composite of Handan, Technology Innovation Center of Modified Plastics of Hebei Province, School of Materials Science and Engineering, Hebei University of Engineering, Handan 056038, Hebei, China
[3] Department of Chest Surgery, Handan First Hospital, Handan 056002, Hebei, China

Abstract

A novel magnetic-targeted pH-responsive intelligent drug carrier based on hollow mesoporous structured $NiFe_2O_4$ nanospheres was designed and developed for potential anticancer treatment in the present study. The hollow mesoporous $NiFe_2O_4$ nanospheres were fabricated through a template-free solvothermal approach and the possible formation mechanism of this structure was proposed. The products were investigated comprehensively for their morphology, microstructure, composition and magnetic properties using a wide series of characterization methods. The $NiFe_2O_4$ nanospheres were demonstrated to possess a well-defined spherical morphology, homogeneous particle size distribution, large hollow cavities and abundant mesopores, unique superparamagnetic behavior, high saturation magnetization as well as good biocompatibility. Due to these desirable physicochemical properties, the hollow mesoporous $NiFe_2O_4$ nanospheres were expected to be employed as a potential vehicle for loading and delivering anticancer drug of doxorubicin hydrochloride (DOX). Drug release behavior was evidenced to be controllable and pH-responsive with effective DOX release of 73.1% and 58.8% in acidic conditions (pH 4.0 and 5.5), whereas insufficient drug release of 44.7% at a neutral atmosphere (pH 7.4) within 48 h. More importantly, the DOX-loaded $NiFe_2O_4$ nanospheres displayed significant antiproliferation and apoptosis effects on human breast cancer cells (MCF-7), which further indicated the promising potential application of constructed drug delivery nanocarriers in the field of cancer therapy.

Keywords: Template-free, Hollow mesoporous, pH-responsive, Drug delivery, Anticancer treatment

Introduction

With the rapid developments of materials science and nanotechnology, nanomaterials with novel structures and unique functional features have been extensively applied in targeted drug delivery for potential cancer treatment (Tibbitt et al. 2016; Mitchell et al. 2020; Taherian et al. 2021; Tran et al. 2018; Tran and Lee 2018). In recent years, design and establishment of efficient drug delivery systems have attracted increasing attention in both fundamental research and practical applications, and extraordinary efforts have been launched to develop the effective strategies for realization of good targeting ability and controllable drug release properties. A vast variety of nanomaterials have been fabricated and investigated as smart drug delivery systems with different external stimuli, such as physical stimuli (mechanical stress, temperature, electrical, magnetic, light), chemical stimuli (pH, solvent, ions, redox), biological stimuli (enzymes, glucose, inflammation) and dual or multi-triggered stimuli (Liu et al. 2014; Kang and Bae 2003; Ju et al. 2009; Ling et al. 2022; Tran and Lee 2021; Tran et al. 2020; Xie et al. 2020). Magnetic nanomaterials have been deemed as fascinating and promising candidates for stimuli-responsive targeted drug delivery systems through magnetic sensitive responses under different physiological pH environments, achieving multiple targeting functionalization, attaining extended circulation time, decreasing the frequency or dose of drugs, and ultimately increasing the patient compliance (Veiseh et al. 2010; Fuentes-García et al. 2021; Htwe et al. 2022).

Among the various magnetic nanoparticles developed for nanomedicine, $NiFe_2O_4$ nanoparticles have demonstrated great promise in widespread biomedical applications due to their strong magnetic responsiveness, favorable toxicity profile and enhanced tumor targeting efficiency (Khan et al. 2021). In particular, hollow structured $NiFe_2O_4$ nanoparticles are expected to hold many intrinsic advantages including large cavity volume, low density, high surface area and controllable morphology as compared to their bulk counterparts, which make them highly attractive for targeted drug delivery to selectively deliver large amounts of therapeutic agents to the target site without destroying surrounding healthy cells (Lima et al. 2017; Yan et al. 2018). In recent years, different approaches have been developed for controlled fabrication of hollow magnetic nanoparticles with desirable morphology, chemical composition and structural complexity (Wang et al. 2011, 2010; Mohammadi Ziarani et al. 2019). Xu et al. (2013) reported uniform hollow magnetic supraparticles that prepared through a one-pot microwave irradiation reaction using casein micelle as soft templates. The yielded hollow magnetic supraparticles can be served as smart carrier vehicles to deliver the anticancer doxorubicin hydrochloride (DOX) to cancer cells. Drug release experiments revealed that the release of DOX from the obtained nanocarrier was pH-responsive manner. About 83% of DOX was released at acidic conditions within 48 h whereas the release of DOX was only 18% at neutral environment. Zhang et al. (2014) synthesized hollow multi-shell $CoFe_2O_4$ nanospheres by means of a solvothermal process and subsequent annealing treatment with the assist of carbon spheres templates. Experimental results showed that the resultant hollow multi-shell $CoFe_2O_4$ nanospheres exhibited enhanced drug-loading capacity and sustained drug release properties of ibuprofen (IBU). Li and coworkers (2015) fabricated the hollow Fe_3O_4 magnetic nanoparticles for the multifunctional applications in thermal responsive controlled drug delivery and dual-modal bioimaging. The

hollow nanoparticles were synthesized via a combined three-step method by using polystyrene nanoparticles as hard templates via sacrificial template technique with post-heat treatment. Hydrophobic paclitaxel (PTX) and hydrophilic DOX as the anticancer model drugs were loaded into the nanocarrier in their report. The obtained drug carrier system showed highly sensitive thermal response when exposure to an alternating current magnetic field for magnetically switchable drug delivery. Although unremitting efforts have been made by the researchers to design and fabricate a variety of types of hollow magnetic nanoparticles, the current used preparation methods usually involve the removal of template objects, complicated experiment procedures and time-consuming processes. At present, it remains a considerable challenge for direct synthesis of hollow magnetic nanoparticles without adding additional templates, which is preferred in practical applications due to the simple fabrication, low production cost and ease of applicability.

In this study, hollow mesoporous structured $NiFe_2O_4$ nanospheres as a promising drug delivery vehicle for loading DOX were fabricated through a facile solvothermal approach without adding any templates. The morphology and size, crystal structure, chemical composition, porosity information, magnetic properties, drug-loading capacity, controlled release characteristics and in vitro cytotoxicity of the as-prepared $NiFe_2O_4$ nanospheres were extensively characterized by using different techniques. The resultant $NiFe_2O_4$ nanospheres can serve as an effective drug delivery system with high drug-loading capacity and pH-responsive drug release performance. Therefore, this work would provide a unique opportunity for handling the complex tumor microenvironment and other challenging applications.

Experimental methods

Materials

All solvents and reagents were of commercial origin and employed without further treatment. Iron(III) chloride hexahydrate ($FeCl_3{\cdot}6H_2O$), nickel(II) chloride hexahydrate ($NiCl_2{\cdot}6H_2O$), urea, ethylene glycol (EG) and dimethyl sulfoxide (DMSO) were purchased from Shanghai Chemical Reagent Company (China). Doxorubicin hydrochloride (DOX) was achieved from J&K Scientific (China). The human breast cancer cells (MCF-7) and MTT solution (5 mg/mL) were received from Mingjing Biology (China). Minimum essential medium (MEM) with 1% non-essential amino acids (NEAA) and insulin was obtained from PriCells (China). Fetal bovine serum (FBS) was obtained from Peak Serum (USA). Penicillin/streptomycin mixed solution (100X double antibody) and trypsin–EDTA solution (0.25% trypsin, 0.02% EDTA) were bought from Beyotime Biotechnology (China).

Synthesis of hollow mesoporous $NiFe_2O_4$ nanospheres

The synthesis experiment of hollow mesoporous $NiFe_2O_4$ nanospheres was performed through a one-step solvothermal method. Typically, 4 mmol of $FeCl_3{\cdot}6H_2O$ and 2 mmol of $NiCl_2{\cdot}6H_2O$ were dispersed in 40 mL of EG under vigorous stirring. After the metal salts were dissolved completely, 140 mmol of urea was introduced into the above solution under continuous stirring for at least 30 min. Subsequently, the mixture suspension was decanted into a Teflon-lined autoclave, and then the autoclave was sealed carefully and maintained at a temperature of 200 °C for 12 h in an electric oven statically. Upon

completion of the hydrothermal reaction, the autoclave was allowed to naturally cool down to room temperature in air. The final collected black precipitants were washed and dried for further use and characterization.

In vitro *drug loading and release of DOX*

In this study, DOX as the model drug was incorporated into the hollow mesoporous $NiFe_2O_4$ nanospheres. In a typical loading process, 100 mg of $NiFe_2O_4$ nanospheres were dispersed in 50 mL of deionized water and the suspension was sonicated for 20 min. Immediately after sonication, 10 mL of an aqueous solution containing DOX (1 mg/mL) was added into the $NiFe_2O_4$ nanospheres based dispersion. The above-mixed solution was placed in the dark under the slow stirring condition overnight. Afterwards, the separation of DOX-loaded $NiFe_2O_4$ nanospheres was achieved through centrifuging the solution at a speed of 5000 rpm for 30 min and subsequently rinsed with water several times to exclude the unbonded and weakly adsorbed DOX. The drug-loading content was acquired based on the absorbance of supernatant at the working wavelength of 479 nm by using a UV–vis spectrometer (TU-1901, Beijing General).

In vitro release behaviors of DOX from $NiFe_2O_4$ nanospheres were evaluated in PBS solutions with different physicochemical conditions (pH 4.0, 5.5 and 7.4) at 37 °C. Briefly, 10 mg of freshly prepared DOX-loaded nanospheres were suspended in the buffer solution (10 mL) followed by the sonication for 10 min to form a uniform dispersion. Then the dispersion was sealed immediately into a dialysis bag (cut-off $M_n = 14{,}000$) and immersed in a conical flask containing 10 mL of same pH value of PBS solution under a sustained shaking (100 r/min) at body temperature. At predetermined time intervals, 5 mL of external buffer solution was discarded for analysis and replenished with the same amount of preheated PBS solution. The content of DOX in each withdrawn aliquot was measured by the UV–vis techniques at the corresponding absorbance.

In vitro *cytotoxicity*

The MCF-7 cells were cultured in MEM cell culture media including 1% NEAA supplemented with 10% FBS, 0.01 mg/mL insulin, 1% antibiotic mixture composed of penicillin and streptomycin. The cells were maintained in a temperature-controlled humidified incubator with constant settings of 5% CO_2 and 37 °C. Once the MCF-7 cells grew to approximately 90% confluence on plates, they were passaged by trypsinization with 0.25% trypsin–EDTA solution and incubated at 37 °C for further 5 min to completely detach cells from the culture flask. Subsequently, the MCF-7 cells were cultured in triplicate with DOX-loaded $NiFe_2O_4$ nanospheres and $NiFe_2O_4$ nanospheres at a series of sample concentrations. After incubation for 24 h or 48 h, the detailed morphologic changes of MCF-7 cells were characterized through an inverted biological optical microscope (BLD-200, Kexin) and the cell viability was assessed based on the standard MTT assays. After the treatment was completed, 20 μL of MTT solution was added to each well of the culture plate and the reaction continued for another 4 h. The medium containing MTT was gently taken out and 80 μL of DMSO was added to completely dissolve the MTT formazan crystals generated by living cells. The optical density was measured at a working absorbance of 490 nm on a universal microplate spectrophotometer (ELx800, Bio-Tek).

Characterization

The morphologic and microstructural examination was performed by a field emission scanning electron microscope (FESEM, FEG 250, Quanta) and a transmission electron microscope (TEM, G2 F20, Tecnai). The investigation of crystal structure was conducted on an X-ray diffractometer (XRD, Dmax-Ultima^{+}, Rigaku) with Cu K_{α} radiation at 0.154 nm. X-ray photoelectron spectroscopy (XPS) spectra were gained with a high-performance spectrometer (Escalab 250Xi, Thermo Fisher Scientific) equipped with a monochromatic Al K_{α} X-ray source. Specific surface area and pore size distribution of samples were determined form the nitrogen adsorption/desorption isotherms that acquired using a volumetric adsorption apparatus (ASAP 2010, Micromeritics) at liquid nitrogen temperature of 77 K. The characterizations of magnetic properties were performed on a physical property measurement system (PPMS, DynaCool, Quantum Design) at room temperature.

Results and discussion

SEM was adopted to characterize the information of morphology and structure of the fabricated $NiFe_2O_4$ nanomaterials. The representative SEM micrographs are shown in Fig. 1. As indicated in the low magnification SEM images (Fig. 1a, b), it was apparently

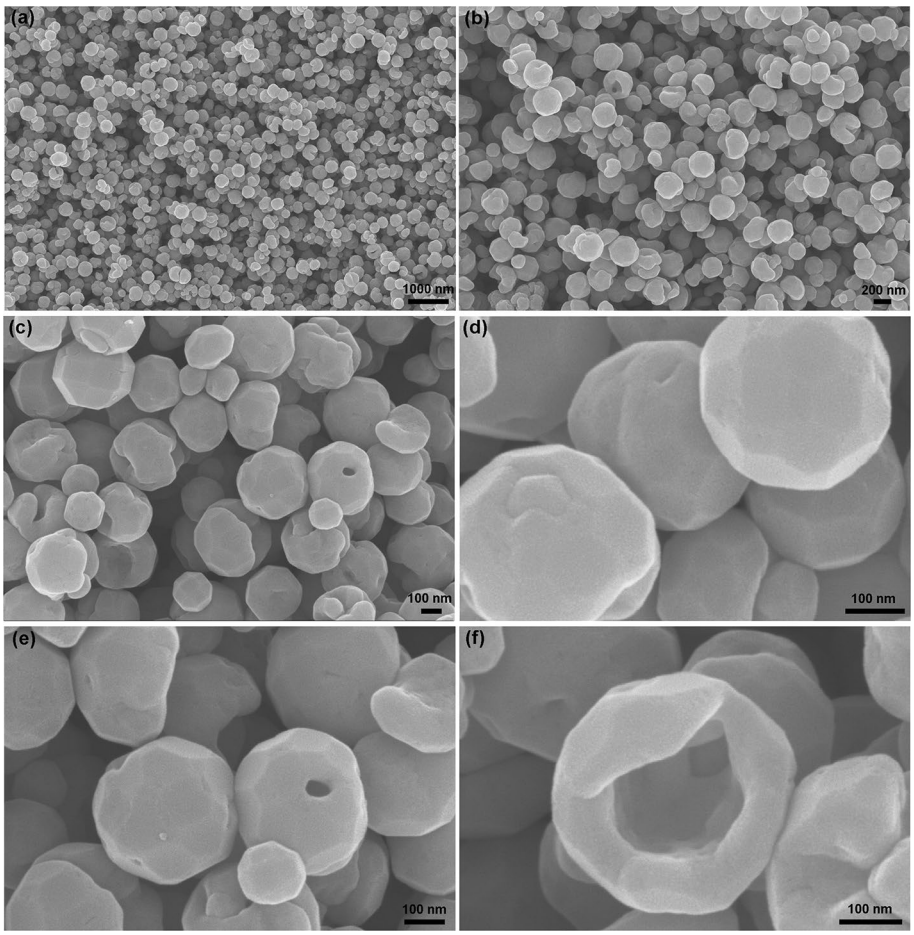

Fig. 1 SEM images of hollow mesoporous $NiFe_2O_4$ nanospheres at different magnifications

demonstrated the products were constituted principally by large amounts of submicronic spherical $NiFe_2O_4$ particles with relatively uniform particle size and uniform dispersion. Figure 1c and d at higher magnifications reveals the further details of surface morphology for $NiFe_2O_4$ nanospheres. It was evident that the $NiFe_2O_4$ nanospheres exhibited fascinating angular and crumpled surfaces, which were markedly distinct from those of the previously reported $NiFe_2O_4$ micro/nanostructures (Sethi et al. 2020; Toghan et al. 2022; Hoghoghifard and Moradi 2022). Furthermore, the partially enlarged SEM images (Fig. 1e, f) showed the presence of holes, cavities and hollow spaces in the $NiFe_2O_4$ nanospheres, indicating the hollow mesoporous structures can be achieved by a one-step solvothermal approach. The fabricated $NiFe_2O_4$ nanospheres were intensively investigated by TEM characterizations. The representative TEM images of $NiFe_2O_4$ nanospheres in Fig. 2 showed that the as-prepared products were hollowed in structure, which was able to accommodate a large quantity of drugs. It was noteworthy that dozens of irregularly shaped nanopores were randomly distributed over the surface of $NiFe_2O_4$ nanospheres, confirming the presence of mesoporous structures. The average particle size of $NiFe_2O_4$ nanospheres was assessed to be approximately 207.3 nm by measuring the diameters of nanospheres in the TEM image using ImageJ software.

Figure 3 displays the schematic formation mechanism of hollow mesoporous $NiFe_2O_4$ nanospheres and their potential as drug delivery systems for cancer treatment application. Urea was used as the alkali source in this solvothermal process, which was decomposed into CO_2 and NH_3 bubbles at an elevated reaction temperature. The OH^- was formed as a result from the combination of NH_3 and H_2O. Both Fe^{3+} and Ni^{2+} cationic ions were reacted with sufficient OH^- and co-precipitated into

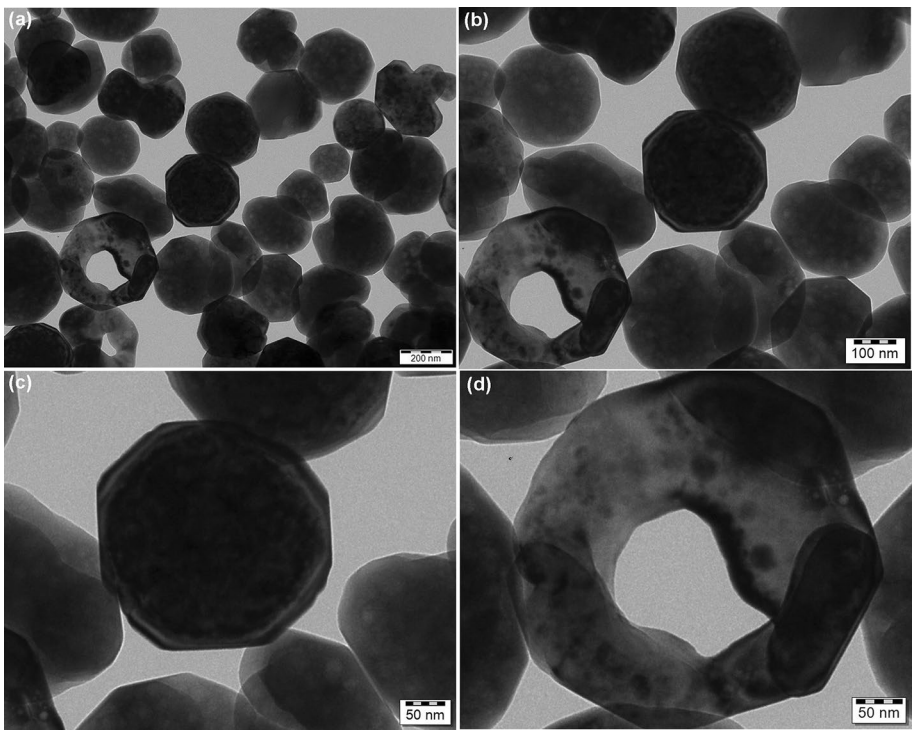

Fig. 2 TEM images of hollow mesoporous $NiFe_2O_4$ nanospheres at different magnifications

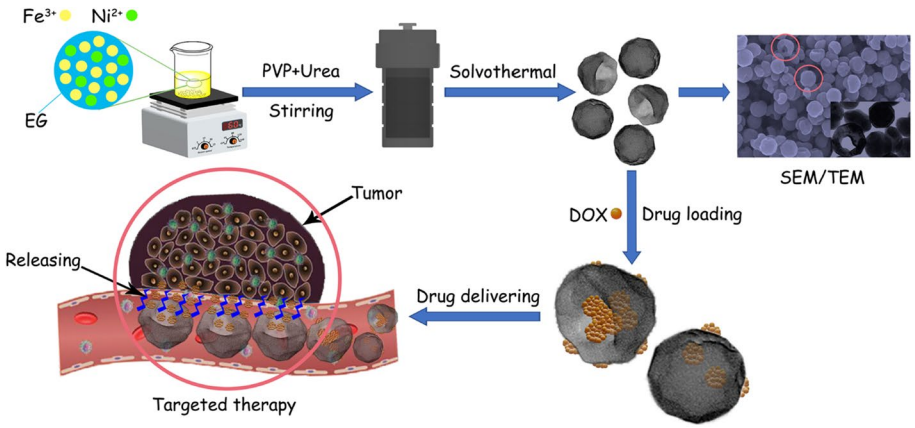

Fig. 3 Schematic diagram of fabrication process and drug delivery application of hollow mesoporous $NiFe_2O_4$ nanospheres

hydroxides, and consequently $NiFe_2O_4$ nanocrystals were produced after the thermal dehydration of hydroxides. The CO_2 and NH_3 bubbles as soft templates probably played an important role in the formation of hollow structures. The released microbubbles of CO_2 and NH_3 were arrested in the reaction medium at a saturated steam pressure owing to the limited capacity of the autoclave in the presence of excessive amount of urea added. These detained microbubbles could be served as the nucleation centers and the formed primary nanocrystals aggregated around the gas–liquid interface due to the minimization of interfacial energy, and finally the hollow $NiFe_2O_4$ nanospheres were obtained with crystal growth and Ostwald ripening process. It should be noted that the hollowing phenomenon was insignificant in this study (Figs. 1, 2), which was probably due to the fact that overabundant microbubbles in this system resulted in intense collision effect in the constrained autoclave (Su et al. 2016; Deng et al. 2011). Additionally, the formation of mesopores on the surface of $NiFe_2O_4$ nanospheres was explained based on the assumption that the electrostatic attractions between urea molecules and PVP chains were acted as the soft templates for assembling similar surfactant structures (Guo et al. 2009). However, the detailed formation mechanism of hollow mesoporous $NiFe_2O_4$ nanospheres remained unclear at the moment. As expected, the existence of large inner cavities and abundant mesoporous pores on the surface of $NiFe_2O_4$ nanospheres would probably make them to be used as a promising candidate for magnetic targeted drug delivery.

Powder XRD measurements were performed to discover the crystallographic information of the obtained $NiFe_2O_4$ nanospheres. The recorded XRD pattern in Fig. 4 revealed a series of intense and argute diffraction signals, indicating the resultant $NiFe_2O_4$ nanospheres possessed high crystallinity. The detected characteristic diffraction peaks were correctly indexed to the crystalline phase structure of $NiFe_2O_4$ centering at (111), (220), (311), (222), (400), (422), (511) and (440) planes, respectively, which were accorded remarkably with the standard data of JCPDS 74-2403. No additional diffraction signals of other crystalline phases or apparent impure phases were demonstrated in this XRD pattern, disclosing the high purity of $NiFe_2O_4$ nanospheres in the present work.

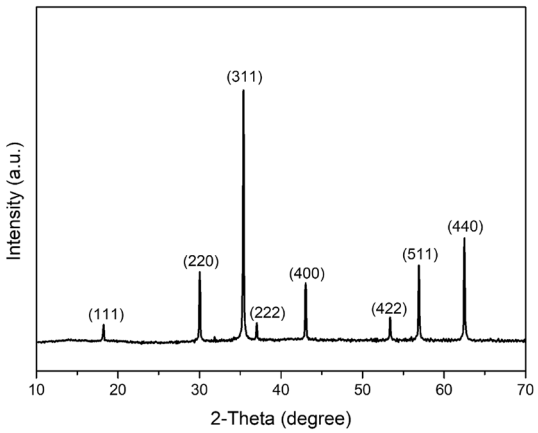

Fig. 4 XRD pattern of hollow mesoporous $NiFe_2O_4$ nanospheres

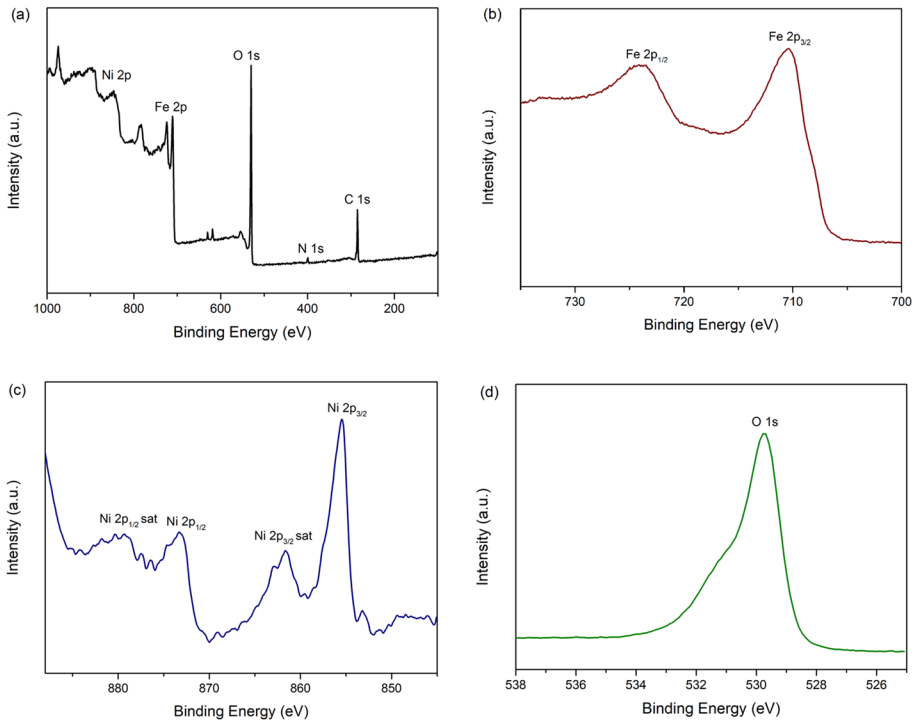

Fig. 5 XPS survey spectrum (**a**) and high-resolution XPS spectra of Fe 2p (**b**), Ni 2p (**c**), O 1 s (**d**) of hollow mesoporous $NiFe_2O_4$ nanospheres

To corroborate the successful synthesis of $NiFe_2O_4$ nanospheres, the XPS characterizations were performed for surface composition investigation and chemical state analysis. The survey scan XPS spectrum shown in Fig. 5a evidently revealed the existence of Fe, Ni, O, C and N elements according to the observed binding energy peaks. In the narrow scan XPS spectrum of Fe 2p orbital (Fig. 5b), the prominent peaks located at 710.4 eV and 724.1 eV were ascribed to the core levels of Fe $2p_{3/2}$ and Fe $2p_{1/2}$ of divalent Fe signals, respectively. As illustrated in Fig. 5c, the narrow scan XPS spectrum of Ni 2p orbital contained two major peaks with binding energy values at about 873.4 eV and

855.5 eV accompanied by their corresponding shakeup satellite peaks of 879.8 eV and 861.6 eV, which can be referenced to Ni $2p_{1/2}$ and Ni $2p_{3/2}$ of trivalent Ni signals, respectively (Chen et al. 2019). From the aforementioned results, it was further verified that the $NiFe_2O_4$ nanospheres have been successfully fabricated after the solvothermal process.

The specific surface area and pore size distribution of hollow mesoporous $NiFe_2O_4$ nanospheres were evaluated from nitrogen adsorption–desorption isotherms. As evident from Fig. 6, the recorded isotherms demonstrated representative IV characteristics with a well-defined hysteresis loop at high relative pressures (P/P_o) varying from 0.7 to 1.0, providing evidence for the existence of a massive number of uniform accessible mesopores. The BJH pore size distribution of hollow mesoporous $NiFe_2O_4$ nanospheres is illustrated in the insert of Fig. 6, which was acquired from the adsorption branch of isotherms. It was revealed that the $NiFe_2O_4$ nanospheres typically possessed a narrow pore size distribution centering at 2.2 nm. The specific surface area, average pore size and total volume of pores of the $NiFe_2O_4$ nanospheres were estimated to be about 61.8 m^2/g, 4.24 nm and 0.18 cm^3/g, respectively. As a result, due to the presence of unique mesoporous structures and large pore volume, the resultant $NiFe_2O_4$ nanospheres were capable of accommodating and delivering anticancer drugs.

Room temperature magnetic measurements were carried out to reveal the magnetic properties of hollow mesoporous $NiFe_2O_4$ nanospheres. According to the recorded magnetization curves in Fig. 7, it was demonstrated that the specimens exhibited minimal magnetic hysteresis loops, elucidating the typical superparamagnetic characteristics of the as-prepared $NiFe_2O_4$ nanospheres. The saturation magnetization can be derived from the data analysis of magnetization curves. The value of saturation magnetization of $NiFe_2O_4$ nanospheres was determined to be roughly 86.7 emu/g, promulgating a strong magnetic responsiveness in magnetic field. It has been generally recognized that saturation magnetization and superparamagnetic performance are crucial characteristic parameters for magnetic nanoparticles in related biomedical applications. High saturation magnetization allows the magnetic nanoparticles to be easily separated under an external magnetic field and magnetically guided to tumors and desired tissues for enhancing the delivery efficiency of therapeutic agents. Magnetic nanoparticles are endowed with good redispersion ability in aqueous solution after removal of external

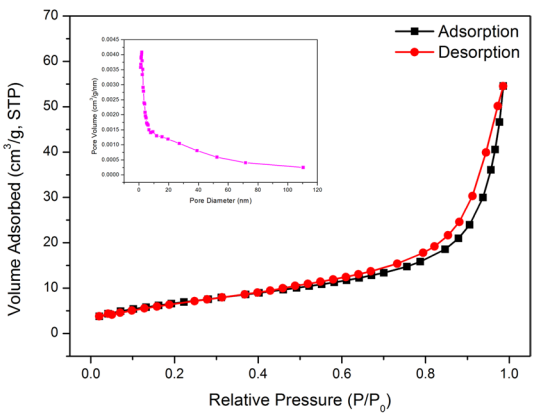

Fig. 6 Nitrogen adsorption–desorption isotherms of hollow mesoporous $NiFe_2O_4$ nanospheres. The inset shows the determined pore size distribution curve

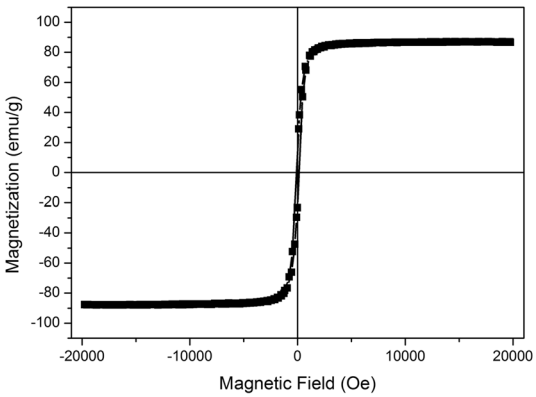

Fig. 7 Magnetization curves of hollow mesoporous $NiFe_2O_4$ nanospheres at room temperature

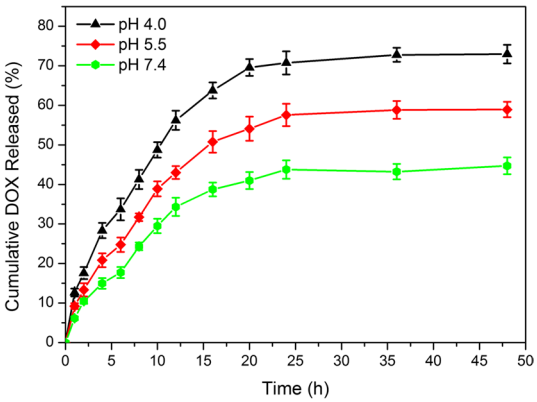

Fig. 8 Cumulative release curves of DOX from hollow mesoporous $NiFe_2O_4$ nanospheres at different pH values of 4.0, 5.5 and 7.4

magnetic field owing to their superparamagnetism, avoiding the possible embolization of capillary vessels resulting from the coagulation and agglomeration of magnetic nanoparticles (Singh and Sahoo 2014; Iafisco et al. 2016).

Due to the unique features of $NiFe_2O_4$ nanospheres such as uniform particle size, typical hollow mesoporous structures, superparamagnetism, high saturation magnetization, the fabricated $NiFe_2O_4$ nanospheres are expected to have a promising application in drug delivery system. A currently used broad spectrum anticancer agent named DOX was introduced to examine the drug-loading capacity and drug release profile of the hollow mesoporous $NiFe_2O_4$ nanospheres. The DOX-loading capacity was estimated to be about 37%. The in vitro DOX release profiles of hollow mesoporous $NiFe_2O_4$ nanospheres were examined in PBS solutions at 37 °C with various pH values (4.0, 5.5 and 7.4) simulating the intracellular environment and intracellular compartment (Mura et al. 2013). The recorded drug release profiles in Fig. 8 demonstrated that tolerably low amount of incorporated DOX (44.7%) was released from the hollow mesoporous $NiFe_2O_4$ nanospheres after 48 h of release experiment at a natural condition (pH = 7.4), implying inferior premature drug release and good structure stability of DOX-loaded $NiFe_2O_4$ nanospheres. In contrast, the encapsulated drug could be released as high as 73.1% and 58.8% in the acidic release buffers with pH values of 4.0 and 5.5 in the same

recording time. The difference in cumulative release amounts at various pH values was mainly assigned to the solubility difference of DOX in aqueous medium and intensity difference in hydrogen-bonding interactions. On one hand, the primary amine groups of DOX were protonated ($pK_a = 8.3$) under acidic conditions, thereby increasing the aqueous solubility of DOX and facilitating the drug release from $NiFe_2O_4$ nanospheres (Tran and Lee 2021; Lim et al. 2011). On the other hand, the hydrogen-bonding interactions between hydroxyl and amine groups of DOX molecules and hydroxyl and carboxyl groups of $NiFe_2O_4$ nanospheres would be weakened even broken under acidic conditions, consequently resulting in an accelerated release of DOX (Tran et al. 2020). Thus, the established hollow mesoporous $NiFe_2O_4$ nanospheres can be employed as outstanding candidates for pH-responsive drug delivery system, which can avoid the burst release of loaded anticancer drugs from drug delivery system during blood circulation while enhance the intracellular drug release inside tumor cells (Kanamala et al. 2016).

For the assessments of DOX-loaded $NiFe_2O_4$ nanospheres in the applications of biomedicine, a preliminary evaluation on anticancer efficiency toward MCF-7 cells was conducted utilizing an MTT assay. As can be found in Fig. 9a, $NiFe_2O_4$ nanospheres in the sample concentration range of 25–150 μg/mL demonstrated ignorable anti-proliferation and inhibition effects on MCF-7 cells with the cell viability maintaining over 90.3% even after co-incubation with $NiFe_2O_4$ nanospheres for 24 h. More significantly, it was worth reminding that DOX-loaded $NiFe_2O_4$ nanospheres significantly decreased the cell viability of MCF-7 cells across the whole concentrations as compared to unloaded $NiFe_2O_4$ nanospheres (Fig. 9b). After 12 h of incubation, the cell viability was 82.4% at the concentration of 50 μg/mL of drug-loaded $NiFe_2O_4$ nanospheres. As the concentration was raised to 150 μg/mL, the cell viabilities were dropped to 53.4% and 50.2% after being incubated for 12 h and 24 h under the same conditions. The results showed that DOX-loaded $NiFe_2O_4$ nanospheres had a marked cytotoxic activity against the MCF-7 cells in a concentration- and time-dependent manner.

Furthermore, biological optical microscopy characterizations were performed to reveal the cell morphology variations of MCF-7 cells in terms of different concentrations after incubation with pure $NiFe_2O_4$ nanospheres for 24 h, as displayed in Fig. 10. After treatment with different concentrations of pure $NiFe_2O_4$ nanospheres (0, 25, 50 and 150 μg/mL), one can find that the MCF-7 cells remained a normal cobblestone-like polygonal morphology with a clear outline and the amounts of living cells were

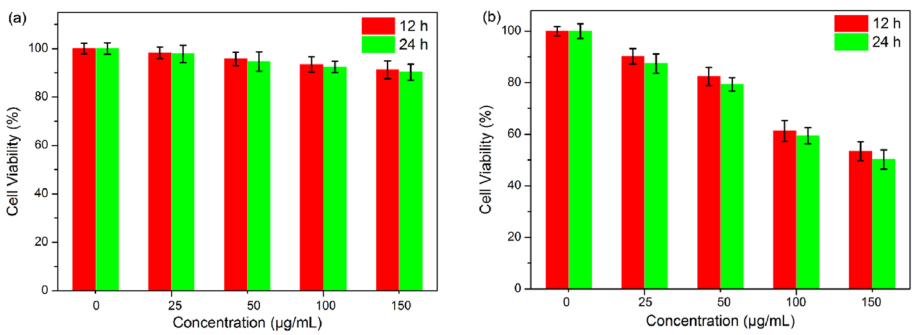

Fig. 9 Cell viability of MCF-7 cells after treatment with hollow mesoporous $NiFe_2O_4$ nanospheres and DOX-loaded $NiFe_2O_4$ nanospheres at different concentrations for 12 h and 24 h

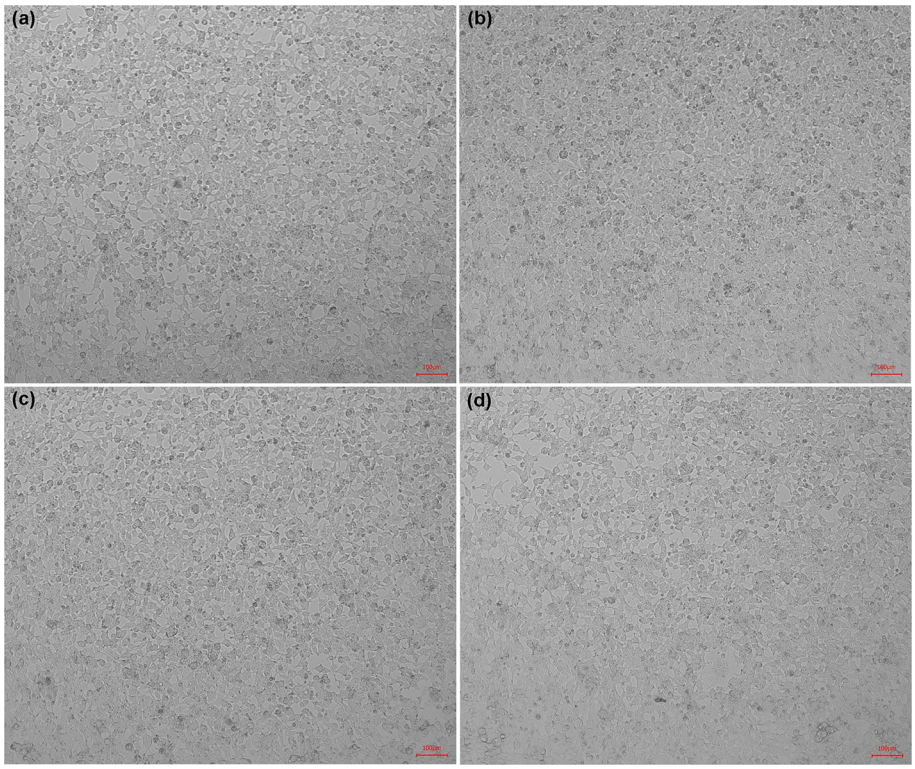

Fig. 10 Optical photos of MCF-7 cells after incubation with hollow mesoporous $NiFe_2O_4$ nanospheres at different concentrations for 24 h

almost unchanged even at the high concentration up to 150 μg/mL. The observations further validated the favorable biocompatibility of $NiFe_2O_4$ nanospheres at all the concentrations examined, which was in accordance with the analysis results obtained from MTT assays. Figure 11 shows the cell morphologies after incubation with DOX-loaded $NiFe_2O_4$ nanospheres changed with concentrations. It was proclaimed that exposure of MCF-7 cells to different concentrations of DOX-loaded $NiFe_2O_4$ nanospheres provoked significant morphology alterations. The MCF-7 cells were found to shrink and retract from their neighboring cells compared to those of pure $NiFe_2O_4$ nanospheres. The numbers of living cells were dramatically reduced with the improvement in used concentrations of DOX-loaded $NiFe_2O_4$ nanospheres, indicating an enhanced antiproliferative and cytotoxic activity toward MCF-7 cells. Based on the above results, the constructed drug delivery system based on hollow mesoporous $NiFe_2O_4$ nanospheres emerged as an alternative candidate for management and treatment of cancers.

Conclusions

In summary, controlled fabrication of hollow mesoporous $NiFe_2O_4$ nanospheres was achieved through a template-free one-step solvothermal approach. Various characterizations revealed that the as-made $NiFe_2O_4$ nanospheres exhibited a uniform particle size, unique hollow mesoporous structure, typical superparamagnetism and high saturation magnetization. Due to these desirable characteristics, the $NiFe_2O_4$ nanospheres were capable of being employed as a drug delivery system with a high drug-loading capacity

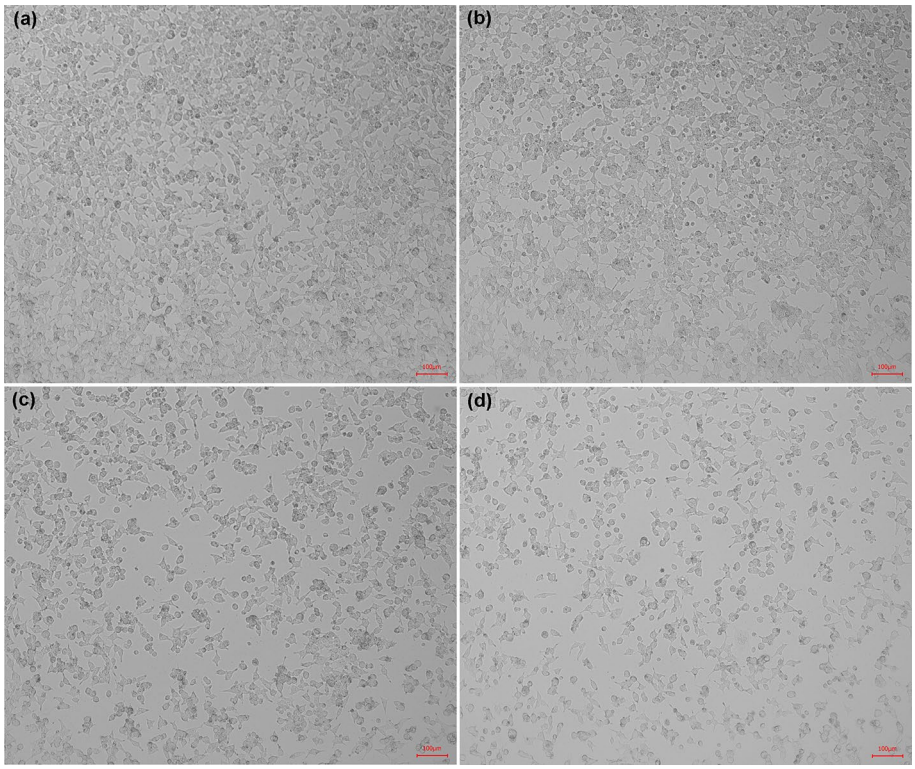

Fig. 11 Optical photos of MCF-7 cells after incubation with DOX-loaded hollow mesoporous $NiFe_2O_4$ nanospheres at different concentrations for 24 h

up to 37% using DOX as a model anticancer drug. Furthermore, the incorporated DOX could be released from DOX-loaded $NiFe_2O_4$ nanospheres in a pH-responsive pathway that the release of DOX was accelerated when exposed to a more acidic microenvironment. Additionally, $NiFe_2O_4$ nanospheres were authenticated to have favorable biocompatibility, while the DOX-loaded $NiFe_2O_4$ nanospheres demonstrated significant inhibitory effects against MCF-7 cells. Consequently, the modified solvothermal strategy without additional templates will undoubtedly afford an effective avenue for construction of well-defined hollow mesoporous $NiFe_2O_4$ nanospheres for controlled drug delivery.

Acknowledgements
The authors are thankful to all members at Cancer Center of Affiliated Hospital and School of Materials Science and Engineering, Hebei University of Engineering.

Author contributions
All authors contribute to the conception, writing and editing of this work. All authors read and approved the final manuscript.

Funding
This work is supported by Science and Technology Research Development Program of Handan (No. 21422083353).

Availability of data and materials
The authors declare that all data supporting the findings of this study are available within the article or from the corresponding author upon reasonable request.

Declarations

Ethics approval and consent to participate
Not applicable.

Consent for publication
All authors have given approval to the final version of the manuscript.

Competing interests
The authors confirm no competing interests.

Received: 23 February 2023 Accepted: 17 March 2023
Published online: 02 May 2023

References

Chen Z, Gao YT, Mu DZ, Shi HF, Lou DW, Liu SY (2019) Recyclable magnetic $NiFe_2O_4$/C yolk–shell nanospheres with excellent visible-light-Fenton degradation performance of tetracycline hydrochloride. Dalton Trans 48(9):3038–3044
Deng CH, Hu HM, Ge XQ, Han CL, Zhao DF, Shao GQ (2011) One-pot sonochemical fabrication of hierarchical hollow CuO submicrospheres. Ultrason Sonochem 18(5):932–937
Fuentes-García JA, Alavarse AC, de Castro CE, Giacomelli FC, Ibarra MR, Bonvent JJ, Goya GF (2021) Sonochemical route for mesoporous silica-coated magnetic nanoparticles towards pH-triggered drug delivery system. J Mater Res Technol 15:52–67
Guo SJ, Li D, Zhang LX, Li J, Wang E (2009) Monodisperse mesoporous superparamagnetic single-crystal magnetite nanoparticles for drug delivery. Biomaterials 30(10):1881–1889
Hoghoghifard S, Moradi M (2022) Influence of annealing temperature on structural, magnetic, and dielectric properties of $NiFe_2O_4$ nanorods synthesized by simple hydrothermal method. Ceramics Int 48(12):17768–17775
Htwe AT, Maung MTM, Naing Z (2022) Synthesis of chitosan-coated magnetite nanoparticles using co-precipitation method for copper(II) ions removal in aqueous solution. World J Eng 19(5):726–734
Iafisco M, Drouet C, Adamiano A, Pascaud P, Montesi M, Panseri S, Sarda S, Tampieri A (2016) Superparamagnetic iron-doped nanocrystalline apatite as a delivery system for doxorubicin. J Mater Chem B 4(1):57–70
Ju XJ, Liu L, Xie R, Niu CH, Chu LY (2009) Dual thermo-responsive and ion-recognizable monodisperse microspheres. Polymer 50:922–929
Kanamala M, Wilson WR, Yang MM, Palmer BD, Wu ZM (2016) Mechanisms and biomaterials in pH-responsive tumour targeted drug delivery: a review. Biomaterials 85:152–167
Kang SI, Bae YH (2003) A sulfonamide based glucose-responsive hydrogel with covalently immobilized glucose oxidase and catalase. J Control Release 86:115–121
Khan AU, Chen L, Ge GL (2021) Recent development for biomedical applications of magnetic nanoparticles. Inorg Chem Commun 134:108995
Li JH, Hu Y, Hou YH, Shen XK, Xu GQ, Dai LL, Zhou J, Liu Y, Cai KY (2015) Phase-change material filled hollow magnetic nanoparticles for cancer therapy and dual modal bioimaging. Nanoscale 7(19):9004–9012
Lim EY, Huh YM, Yang J, Lee K, Suh JS (2011) pH-Triggered drug-releasing magnetic nanoparticles for cancer therapy guided by molecular imaging by MRI. Adv Mater 23:2436–2442
Lima DR, Jiang N, Liu X, Wang JL, Vulcani VAS, Martins A, Machado DS, Landers R, Camargo PHC, Pancotti A (2017) Employing calcination as a facile strategy to reduce the cytotoxicity in $CoFe_2O_4$ and $NiFe_2O_4$ nanoparticles. ACS Appl Mater Interfaces 9:39830–39838
Ling JJ, Jiang YM, Yan SY, Dang H, Yue H, Liu KL, Kuang LH, Liu XX, Tang H (2022) A novel pH- and glutathione-responsive drug delivery system based on in situ growth of MOF199 on mesoporous organic silica nanoparticles targeting the hepatocellular carcinoma niche. Cancer Nanotechnol 13:32
Liu J, Huang Y, Kumar A, Tan A, Jin SH, Mozhi A, Liang XJ (2014) pH-Sensitive nano-systems for drug delivery in cancer therapy. Biotechnol Adv 32(4):693–710
Mitchell MJ, Billingsley MM, Haley RM, Wechsler ME, Peppas NA, Langer R (2020) Engineering precision nanoparticles for drug delivery. Nat Rev Drug Discovery 20(2):1471–1776
MohammadiZiarani G, Malmir M, Lashgari N, Badiei A (2019) The role of hollow magnetic nanoparticles in drug delivery. RSC Adv 9(43):25094–25106
Mura S, Nicolas J, Couvreur P (2013) Stimuli-responsive nanocarriers for drug delivery. Nat Mater 12(11):991–1003
Sethi M, Shenoy US, Muthu S, Bhat DK (2020) Facile solvothermal synthesis of $NiFe_2O_4$ nanoparticles for high-performance supercapacitor applications. Front Mater Sci 14:120–132
Singh A, Sahoo SK (2014) Magnetic nanoparticles: a novel platform for cancer theranostics. Drug Discov Today 19(4):474–481
Su MH, He C, Shih K (2016) Facile synthesis of morphology and size-controlled α-Fe_2O_3 and Fe_3O_4 nano-and micro-structures by hydrothermal/solvothermal process: The roles of reaction medium and urea dose. Ceram Int 42:14793–14804
Taherian A, Esfandiari N, Rouhani S (2021) Breast cancer drug delivery by novel drug-loaded chitosan-coated magnetic nanoparticles. Cancer Nanotechnol 12:15
Tibbitt MW, Dahlman JE, Langer R (2016) Emerging frontiers in drug delivery. J Am Chem Soc 138(3):704–717
Toghan A, Khairy M, Kamar EM, Mousa MA (2022) Effect of particle size and morphological structure on the physical properties of $NiFe_2O_4$ for supercapacitor application. J Mater Res Technol 19:3521–3535
Tran VA, Lee SW (2018) A prominent anchoring effect on the kinetic control of drug release from mesoporous silica nanoparticles (MSNs). J Colloid Interface Sci 510:345–356
Tran VA, Lee SW (2021) pH-triggered degradation and release of doxorubicin from zeolitic imidazolate framework-8 (ZIF8) decorated with polyacrylic acid. RSC Adv 11(16):9222–9234

Tran AV, Shim K, Thi TT, Kook JK, An SSA, Lee SW (2018) Targeted and controlled drug delivery by multifunctional mesoporous silica nanoparticles with internal fluorescent conjugates and external polydopamine and graphene oxide layers. Acta Biomater 74:397–413
Tran VA, Vo VG, Shim K, Lee SW, An SSA (2020) Multimodal mesoporous silica nanocarriers for dual stimuli-responsive drug release and excellent photothermal ablation of cancer cells. Int J Nanomed 15:7667–7685
Veiseh O, Gunn JW, Zhang M (2010) Design and fabrication of magnetic nanoparticles for targeted drug delivery and imaging. Adv Drug Deliv Rev 62(3):284–304
Wang ZY, Luan DY, Li CM, Su FB, Madhavi S, Boey FYC, Lou XW (2010) Engineering nonspherical hollow structures with complex interiors by template-engaged redox etching. J Am Chem Soc 132:16271–16277
Wang Y, Zhu QS, Tao L (2011) Fabrication and growth mechanism of hierarchical porous Fe_3O_4 hollow sub-microspheres and their magnetic properties. CrystEngComm 13(14):4652–4657
Xie XT, Zhang L, Zhang WJ, Tayebee R, Hoseininasr A, Vatanpour HH, Behjati Z, Li SY, Nasrabadi M, Liu LY (2020) Fabrication of temperature and pH sensitive decorated magnetic nanoparticles as effective biosensors for targeted delivery of acyclovir anti-cancer drug. J Mol Liq 309:113024
Xu S, Yin BR, Guo J, Wang CC (2013) Biocompatible hollow magnetic supraparticles: ultrafast microwave-assisted synthesis, casein-micelle-mediated cavity formation and controlled drug delivery. J Mater Chem B 1(33):4079–4087
Yan F, Guo D, Zhang S, Li CY, Zhu CL, Zhang XT, Chen YJ (2018) An ultra-small $NiFe_2O_4$ hollow particle/graphene hybrid: fabrication and electromagnetic wave absorption property. Nanoscale 10(6):2697–2703
Zhang LX, Sun YX, Jia WB, Ma SS, Song B, Li Y, Jiu HF, Liu JW (2014) Multiple shell hollow $CoFe_2O_4$ spheres: Synthesis, formation mechanism and properties. Ceram Int 40:8997–9002

Publisher's Note